

Coordinated Chassis Control Based on Vehicle Lateral Acceleration Using Fuzzy Logic Control

{A. Elhefnawy, A. M. Sharaf, H. Ragheb, S. Hegazy}^{*}

Abstract: This paper presents an advanced coordination of integrated control system which consist of three different controllers namely Electronic Stability Control (ESC), Active Front Steering (AFS), and Active Suspension (AS) using Fuzzy Logic Control (FLC) in order to improve vehicle handling, cornering stability, and rollover prevention with anti-lock braking system (ABS) to avoid wheel locking during generating differential braking by ESC control. Based on a well-developed and validated fourteen degrees of freedom full vehicle model with non-linear tire characteristics, a reference yaw-roll plane vehicle model is introduced to compare and therefore control the yaw rate, side slip angle, and roll angle of the vehicle body. For rollover prevention indices, the dynamic load transfer ratio is defined to check the effectiveness of the proposed controller.

The Coordination chassis control is based on the lateral acceleration value as input to FLC, and the outputs are the increment factors to the three controllers varying from zero to one. Three membership functions are chosen to represent the lateral acceleration as input to the supervisor controller, to define the control authority for each actuator. The universe of discourse for each membership function is selected according to the study of the effect of each controller stand alone in vehicle performance.

The numerical modelling is carried out through the MATLAB / Simulink environment which suits the control and optimization process. Different standard test maneuvers namely J-turn, fishhook, and double lane change have been carried out by considering standard test maneuvers with different driving speeds. The simulation results are compared during three cases namely, the uncontrolled system, the combined controller, and the proposed coordinated controller. The results show a substantial improvement of the vehicle stability in terms of vehicle lateral acceleration, side slip angle, yaw rate, roll angle, and the for the developed coordinated controller compared to combined controller or the conventional system without control.

Keywords: Active Front Steering (AFS), Electronic Stability Control (ESC), Active Suspension (AS), Fuzzy Logic Control, Coordinated Control.

Nomenclature

a, b	Position of the C.G of vehicle from front and rear wheel [m]
$C_{f, r}$	Front/Rear suspension-damping coefficient [N.s/m]
$C_{\alpha f, \alpha r}$	Front/Rear tires cornering stiffness [N/rad]
F_{Xi}, F_{Yi}, F_{Zi}	Tire forces stated at vehicle frame of orientation [N]
F_{xi}, F_{yi}, F_{zi}	Tire forces stated at wheel frame systems [N]

^{*} Egyptian Armed Forces, Egypt.

g	Gravity acceleration [m/s ²]
I_{xx}, I_{yy}, I_{zz}	Vehicle sprung mass moment of inertia [kg.m ²]
I_{xy}, I_{yz}, I_{zx}	Vehicle sprung mass product moment of inertia [kg.m ²]
I_{wi}	Wheels Mass moment of inertia [kg.m ²]
$K_{f,r}$	Front/Rear suspension spring stiffness coefficient [N/m]
L	Distance between front and rear axle (wheelbase) [m]
M_{B_i}	Braking torque applied at each wheel [N.m]
M_{D_i}	Driving torque applied at each wheel hub [N.m]
M_b	Body mass of vehicle [kg]
M_t	Total mass of vehicle [kg]
M_{wi}	Unsprung mass at each wheel [kg]
M_X, M_Y, M_Z	Net moments affecting the vehicle body [N.m]
$\dot{\phi}, \dot{\theta}, \dot{\psi}$	(Roll, pitch and yaw) rotating velocities [rad/s]
$\ddot{\phi}, \ddot{\theta}, \ddot{\psi}$	(Roll, pitch and yaw) rotating acceleration [rad/s ²]
r_{di}	Dynamic rolling radius of each wheel [m]
t_{rf}, t_{rr}	Front and rear axle Wheel track [m]
$\dot{x}, \dot{y}, \dot{z}$	(Forward, lateral and vertical) Translational velocities stated at local frame of reference [m/s]
$\ddot{x}, \ddot{y}, \ddot{z}$	(Forward, lateral and vertical) Translational acceleration stated at local frame of reference [m/s ²]
Z_{bi}, \dot{Z}_{bi}	Vertical velocities and acceleration at corners [m/s], [m/s ²]
$Z_{wi}, \dot{Z}_{wi}, \ddot{Z}_{wi}$	Position, velocity and acceleration of the wheel hub vertical [m], [m/s], [m/s ²]
ϕ, θ, ψ	(Roll, pitch and yaw) sprung mass angular displacement [rad]
$\omega_i, \dot{\omega}_i$	Wheel angular speed and acceleration [rad/s], [rad/s ²]

Introduction

Vehicle subsystems control has established ample consideration for more than three decades both academically and experimentally. The majority of these systems are based on regulating the tire forces in both longitudinal and lateral directions such as *Acceleration Slip Regulation* (ASR) [1], *Active Front Steering* (AFS) [2], *Electronic Stability Control* (ESC) [3, 4], *Anti-lock Braking System* (ABS) [5], and *Active Suspension* (AS) [6]. It is widely recognized that, ESC-based systems have been showed very successfully in stability recovery with consideration of disturbing the forward dynamics of vehicle, and maybe affecting unwanted forward decelerations. Electronic stability control (ESC), is the development of anti-lock braking system (ABS), which considered assisting vehicle user by maintaining direction control of the vehicle during emergency cornering, speedy run, and driving on slippery roads. Up till now, the (ESC) is the most active commercial device for rollover preclusion. Commonly, Untripped rollover implicates a vehicle is out of control due to high lateral acceleration to yaw.

Recently, there is a tendency of combining different active subsystems to additional improve in vehicle stability, handling, and rollover prevention. As mentioned by Hac and Bodie [7], when a vehicle is fitted out with numerous controllable subsystems, it is significant to coordinate the actions of subsystems controller, so that the last outcome is the best utilization of tyre forces, specifically in driving situations accomplished at the edge of stability zone. The combination design relies on several aspects and has to be considered conflict between actuators, power saving of actuators, and capacities of each actuator like corrective moment or

force. From this view extensive combination methods are considered. A cataloging of accessible and possible combination design for the vehicle control has been presented in [8], which can be systematized as (1) centralized, (2) supervisory, (3) hierarchical, and (4) coordinated control. Combined control of AFS, ESC, and AS has been taken into consideration from many academics [9-15].

Introduced in [9] a fuzzy logic switch controller is used to coordinate between tracking yaw rate (steerability), and bounded lateral velocity (stability) using phase plane method. The expression of Vehicle Dynamics Management is introduced in [10], which was mainly depend on ESC and then add AFS, and AS regarding to three definite modes namely comfort, safety, and shut-down. Introduced in [11] the integration rules rely on side slip estimation, and apply phase plane method to create these rules. Introduced in [12], the authors used the integration of the AFS, AS, ABS, and ESC, every one of these systems has different modes relying on the vehicle dynamics status, the author assumed them seven modes. Introduced in [13] the author add torque vectoring to the previous mentioned in [12], and study the control authority for each of them then used the lateral acceleration value as discrete region to define the control action weighting for each active control system.

Based on the previous work, this paper develops three fuzzy logic controllers for AFS, AS, and ESC, then a new supervisor FLC controller is designed to coordinate the weight of action for each controller regarding to the value of lateral acceleration of the vehicle to improve the vehicle lateral stability, and rollover prevention.

In this paper, a 14-DOF vehicle model incorporating nonlinear tire characteristics is highlighted. The simulation results of the vehicle cornering response during double lane change maneuver are compared with that of highly sophisticated models developed in ADAMS software and well known commercial vehicle dynamic's software such as CarSim. Furthermore, an integrated control system of yaw rate, roll angle, and side slip angle is designed based on the integrated FLC for AFS, AS, and ESC to enhance the vehicle handling, stability, and rollover prevention.

Model Description

A complete full vehicle model, which contains 14 DOF was developed and published by sharaf [16], which used to analyze the vehicle performance in the three translation, and rotational directions and suits the application of control systems. The magic tire formula (Pacejka model) is used. The validation of this model is done by the dynamic test double lane change using ADAMS/Car and CarSim.

Sprung Mass Dynamics

The body mass of the vehicle has 6 DOF, as illustrated in Fig. 1-a, b. deduced on Newton-Euler law, the equations of motion of the body mass can be inscribed as follow [17]:

$$\Sigma F_x = m_t \cdot (\ddot{x} - \dot{y} \cdot \dot{\psi} + \dot{z} \cdot \dot{\theta}) - m_b \cdot [x_G \cdot (\dot{\theta}^2 + \dot{\psi}^2) - y_G \cdot (\dot{\phi} \cdot \dot{\theta} - \ddot{\psi}) - z_G \cdot (\dot{\phi} \cdot \dot{\psi} + \ddot{\theta})] \quad (1)$$

$$\Sigma F_y = m_t \cdot (\ddot{y} - \dot{z} \cdot \dot{\phi} + \dot{x} \cdot \dot{\psi}) - m_b \cdot [y_G \cdot (\dot{\psi}^2 + \dot{\phi}^2) - z_G \cdot (\dot{\theta} \cdot \dot{\psi} - \ddot{\phi}) - x_G \cdot (\dot{\phi} \cdot \dot{\theta} + \ddot{\psi})] \quad (2)$$

$$\Sigma F_z = m_b \cdot (\ddot{z} - \dot{x} \cdot \dot{\theta} + \dot{y} \cdot \dot{\phi}) - m_b \cdot [z_G \cdot (\dot{\phi}^2 + \dot{\theta}^2) - x_G \cdot (\dot{\phi} \cdot \dot{\psi} - \ddot{\theta}) - y_G \cdot (\dot{\theta} \cdot \dot{\psi} + \ddot{\phi})] \quad (3)$$

$$\Sigma M_x = I_{xx} \cdot \ddot{\phi} - (I_{yy} - I_{zz}) \cdot \dot{\theta} \cdot \dot{\psi} + I_{yz} \cdot (\dot{\psi}^2 - \dot{\theta}^2) - I_{zx} \cdot (\dot{\phi} \cdot \dot{\theta} + \ddot{\psi}) + I_{xy} \cdot (\dot{\phi} \cdot \dot{\psi} - \ddot{\theta}) + m_b \cdot y_G \cdot (\ddot{z} - \dot{x} \cdot \dot{\theta} + \dot{y} \cdot \dot{\phi}) - m_b \cdot z_G \cdot (\ddot{y} - \dot{z} \cdot \dot{\phi} + \dot{x} \cdot \dot{\psi}) \quad (4)$$

$$\Sigma M_y = I_{yy} \cdot \ddot{\theta} - (I_{zz} - I_{xx}) \cdot \dot{\phi} \cdot \dot{\psi} + I_{xz} \cdot (\dot{\phi}^2 - \dot{\psi}^2) - I_{xy} \cdot (\dot{\theta} \cdot \dot{\psi} + \ddot{\phi}) + I_{yz} \cdot (\dot{\theta} \cdot \dot{\phi} - \ddot{\psi}) + m_b \cdot z_G \cdot (\ddot{x} - \dot{y} \cdot \dot{\psi} + \dot{z} \cdot \dot{\theta}) - m_b \cdot x_G \cdot (\ddot{z} - \dot{x} \cdot \dot{\theta} + \dot{y} \cdot \dot{\phi}) \quad (5)$$

$$\begin{aligned} \Sigma M_z = & I_{zz} \cdot \ddot{\psi} - (I_{xx} - I_{yy}) \cdot \dot{\phi} \cdot \dot{\theta} + I_{xy} \cdot (\dot{\theta}^2 - \dot{\phi}^2) - I_{yz} \cdot (\dot{\psi} \cdot \dot{\phi} + \ddot{\theta}) + I_{zx} \cdot (\dot{\psi} \cdot \dot{\theta} - \ddot{\phi}) \\ & + m_b \cdot x_G \cdot (\ddot{y} - \dot{z} \cdot \dot{\phi} + \dot{x} \cdot \dot{\psi}) - m_b \cdot y_G \cdot (\ddot{x} - \dot{y} \cdot \dot{\psi} + \dot{z} \cdot \dot{\theta}) \end{aligned} \quad (6)$$

The gross forces (ΣF_x) are the vehicle forces in the forward path, taking into account air resistance and grade resistance, also (ΣF_y), and (ΣF_z) are the gross lateral force, and vertical forces respectively. The external moments of the aforementioned forces about vehicle axis are ($\Sigma M_x, \Sigma M_y, \Sigma M_z$).

Unsprung Mass Dynamics

Eight DOF that represent the unsprung mass dynamics, two for each wheel one for the vertical movement, and the other for wheel spin as shown in Figs. 1-c, d. The equation of motion can be inscribed as follow:

$$m_{w_i} \cdot \ddot{z}_{w_i} = m_{w_i} \cdot g + \underbrace{C_i \cdot (\dot{z}_{b_i} - \dot{z}_{w_i}) + K_i \cdot (z_{b_i} - z_{w_i})}_{\text{Suspension Force (F}_{si})} + F_{z_i}(z) \quad (7)$$

$$I_{w_i} \cdot \dot{\omega}_i = M_{Di} - M_{Ui} - M_{Bi} - (F_{xi} \cdot r_{di}) \quad (8)$$

Tire Forces and Moments

To imitate the real underlying forces of tire, an accurate tire model would be considered in simulation. The Magic Formula MF affords an accurate tire underlying forces estimation in all regions of tire [18], the general form of MF can be stated as follows:

$$y = D \cdot \sin \left[C \cdot \arctan \left(B \cdot x - E (Bx - \arctan Bx) \right) \right] \quad (9)$$

where Y symbolizes the longitudinal force, the lateral force, or the aligning torque, and X is the longitudinal slip ratio. The tire forces in longitudinal and lateral direction are calculated based on wheel longitudinal slip (λ) and slip angle (α).

(B, C, D, E) in equation (9) are the factors of the magic formula are considered based on the force and moment data obtained through experimental testing.

However when the vehicle is cornering, or braking the tyre vertical load will relocation among four wheels due to longitudinal, and lateral acceleration as written in Equation (10).

$$\left. \begin{aligned} F_{z1} &= \frac{b}{2L} m_t \cdot g - \frac{h_g}{2L} m_t \cdot a_x - \frac{bh_g}{2LC} m_t \cdot a_y \\ F_{z2} &= \frac{b}{2L} m_t \cdot g - \frac{h_g}{2L} m_t \cdot a_x + \frac{bh_g}{2LC} m_t \cdot a_y \\ F_{z3} &= \frac{a}{2L} m_t \cdot g + \frac{h_g}{2L} m_t \cdot a_x + \frac{ah_g}{2LC} m_t \cdot a_y \\ F_{z4} &= \frac{a}{2L} m_t \cdot g + \frac{h_g}{2L} m_t \cdot a_x - \frac{ah_g}{2LC} m_t \cdot a_y \end{aligned} \right\} \quad (10)$$

a_x, a_y presents the vehicle body acceleration at longitudinal and lateral direction.

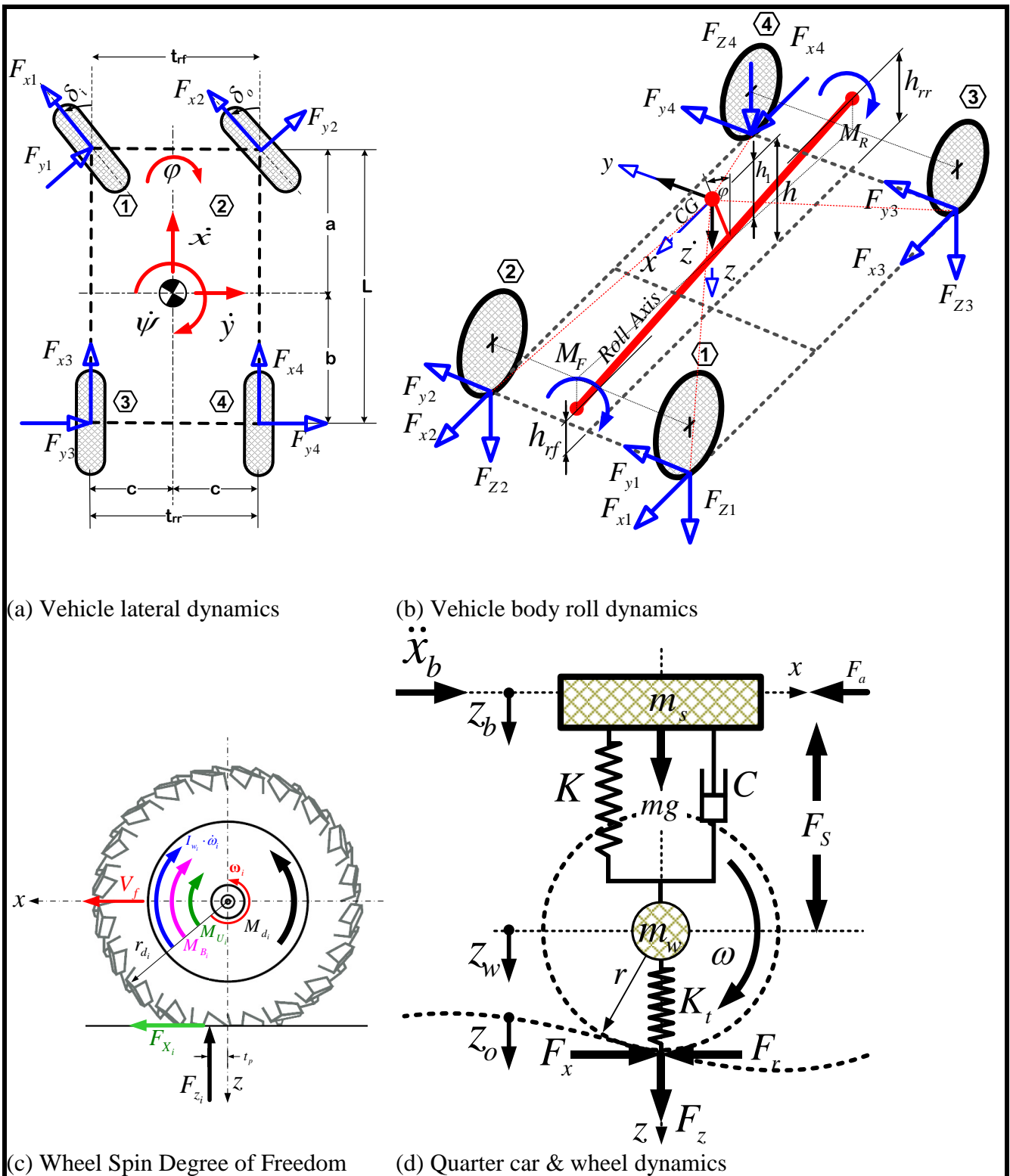


Fig. 1 Full vehicle model dynamics [16]

The model is further validated with an acceptable level of accuracy against the well know commercial packages such as highly complex models created in Adams-Car and medium sophisticated models created in CarSim during double lane change maneuver as shown in Fig. 2.

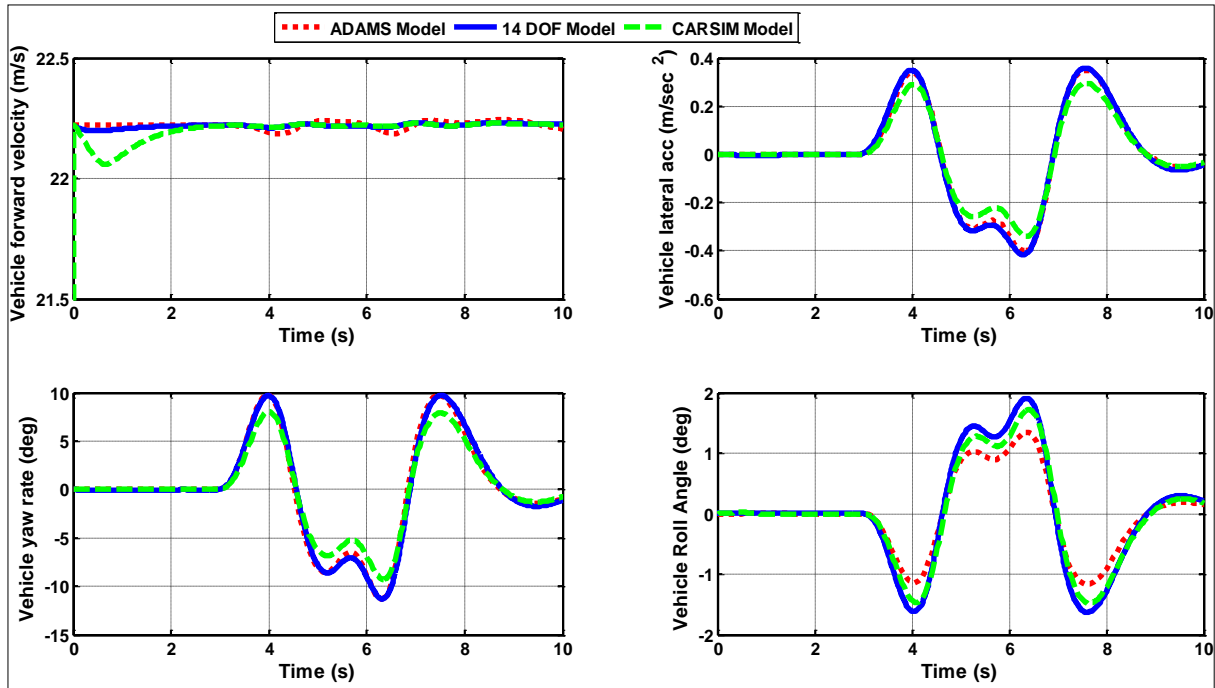


Fig. 2 Validation of full vehicle model with ADAMS and CARSIM

Combined Controller

The meaning of combined control is the physical adding of all active systems in the vehicle. To develop the performance of the vehicle from the points of view like handling, stability, and rollover prevention all the states that represent them should be controlled to track their desired values.

The proposed combined control is consisting of Electronic Stability Control (ESC), Active Front Steering (AFS), and Active Suspension (AS). The overall scheme of the combined controller illustrated in Fig. 3.

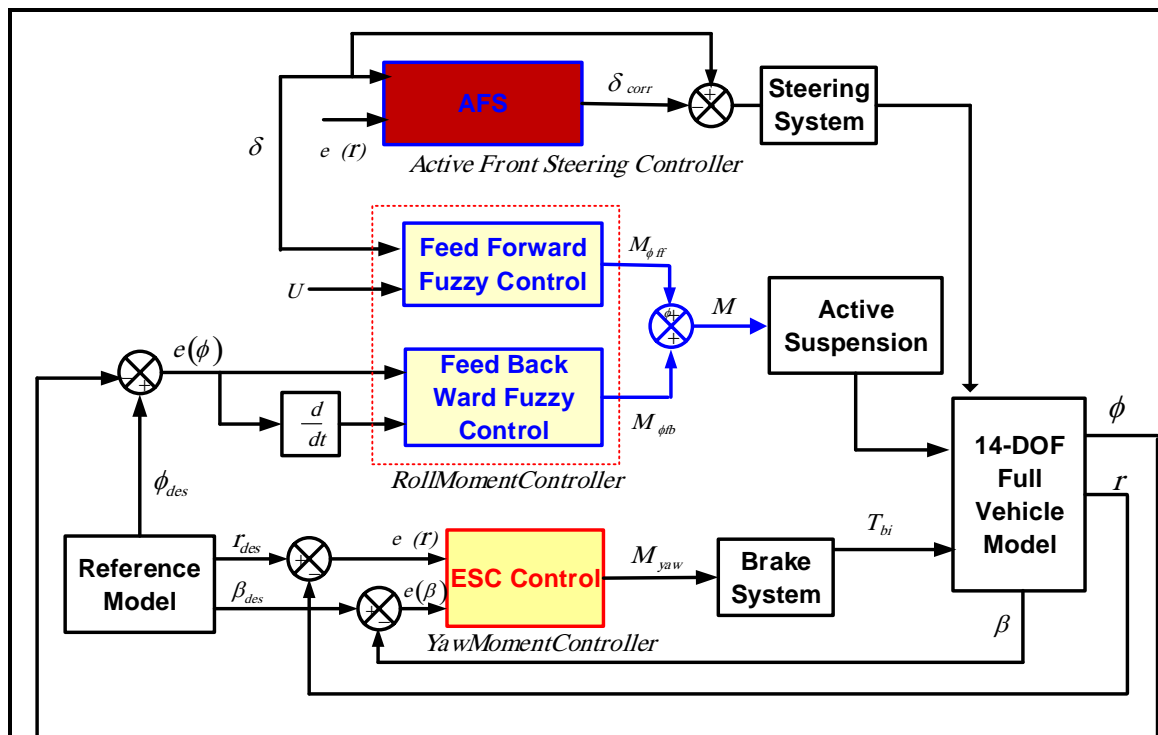


Fig. 3 Block diagram of the combined controller.

As shown in Fig. 3, there are three outputs for the proposed combined controller as follow:-

1. The direct yaw moment M_{yaw} , for ESC controller which takes two parameters as inputs $(e(\dot{\psi}), e(\beta))$ and then converted to differential braking into the left and right sides of the vehicle according to the sign of the yaw moment required.
2. The active roll moment for Active suspension control, this takes four parameters as inputs $\left(\dot{x}, \delta, e(\phi), \frac{d}{dt}e(\phi)\right)$ and then converted to suspension actuators according to the sign of this moment.
3. The corrective steering angle at active front steering control, which takes two parameters as inputs $(e(\dot{\psi}), \delta)$.

The following equation will describe all the inputs and outputs of the combined controller:-

$$\left. \begin{aligned} \text{The Yaw Rate Error :} & \quad e(\dot{\psi}) = \dot{\psi} - \dot{\psi}_{des} \\ \text{The Side Slip Angle Error :} & \quad e(\beta) = \beta - \beta_{des} \\ \text{The Direct Yaw Moment :} & \quad M_{yaw} \\ \text{The Direct Roll Moment :} & \quad M_{roll} \\ \text{The Corrective Steering Angle:} & \quad \delta_{corr} \end{aligned} \right\} \quad (11)$$

A yaw-roll plane vehicle model is used to evaluate the desired yaw rate $(\dot{\psi}_{des})$, and the desired sideslip angle (β_{des}) . The reference of the yaw rate, and side slip angle to the driver's steering wheel angle input δ and forward speed \dot{x} is calculated [19].

$$\dot{\psi}_{des} = \frac{\dot{x}}{\left(L + \frac{M_t \cdot \dot{x}^2 \cdot (b \cdot c_{ar} - a \cdot c_{af})}{2 \cdot c_{af} \cdot c_{ar} \cdot L} \right)} \cdot \delta \quad (12)$$

$$\beta_{des} = \frac{b - \frac{aM_t U^2}{2 \cdot c_{ar} \cdot L} \cdot \delta}{\left(L + \frac{M_t \cdot U^2 \cdot (b \cdot c_{ar} - a \cdot c_{af})}{2 \cdot c_{af} \cdot c_{ar} \cdot L} \right)} \quad (13)$$

Dynamic load transfer ratio LTR_d is used to recognize the rollover of a vehicle, can be simply well-defined as the variance between the load on the right- hand side tyres and the load on the left-hand side tyres of the vehicle, and normalized by the total load, which can be represented by the following equation [20].

$$LTR_d = \frac{F_{z1} + F_{z3} - F_{z2} - F_{z4}}{F_{z1} + F_{z3} + F_{z2} + F_{z4}} \quad (14)$$

From the roll moment equilibrium, LTR_d can be rewritten as follow:-

$$LTR_d = \frac{2M_b}{M_t t_{rf}} \left[(h_r + h_s \cos \phi) \frac{\ddot{y}}{g} + h_s \sin \phi \right] \quad (15)$$

Under ordinary driving situations on a straight path, the tyre loads on both the left and the right are equal, LTR_d is therefore zero. Though, when the vehicle is starting to maneuver in safe rollover range LTR_d is in the range from -1 to 1 . If LTR_d is equivalent to -1 or 1 , this means that the vehicle's left wheels or right wheels have lost contact or are about to lose contact with the ground. In our study we use this parameter to check the effectiveness of the proposed controller.

ABS Controller

The main purpose of the ABS controller is to act as a supervisor controller for the braking force in each wheel individually, which is generated by the direct yaw or roll moment to avoid wheel skidding.

For a braking maneuver, the forward wheel slip ratio is determined by:

$$\lambda = \frac{V_{xw} - V_{rw}}{V_{xw}} \quad (16)$$

From this equation, it can be explained that if the wheel velocity is zero, the wheel slip will equal to one, which is called wheel lock up. However, in normal driving condition the wheel slip will be zero.

Using a 'bang-bang' control constructed upon the difference between real wheel slip and recommended wheel slip, which is considered to be 0.2.

ESC Controller

ESC FLC calculates the yaw moment M_{yaw} as output based on the $e(\beta)$ and $e(\dot{\psi})$ as inputs. As illustrated in Fig. 6, five membership functions are selected to represent the inputs to FLC, which are two trapezoidal and three triangle membership functions. On the other hand, eleven membership functions are selected to represent the output of the controller, which is two trapezoidal, and nine triangle membership functions. The five variables for inputs $e(\beta)$, and $e(\dot{\psi})$ are namely high negative (HN), low negative (LN), zero (ZO), low positive (LP), high positive (HP). The eleven variables for the ESC are (N5, N4, N3, N2, N1, ZO, P1, P2, P3, P4, and P5). The direct yaw moment from fuzzy control is obtained with a scaling factor. The rule base of the ESC FLC is given in Table 2.

Physically, ESC is generated moment which is created due to the variance between the braking force of the left and right side on the front wheels. The sign of ESC moment decide which side will be braked to generate the required moment.

Table 2. Fuzzy Logic Rule Base for ESC and AFS Controller

	HN	LN	ZO	LP	HP
HN	N1	N1	ZO	P1	P1
LN	N2	N2	ZO	P2	P2
ZO	N3	N3	ZO	P3	P3
LP	N4	N4	ZO	P4	P4
HP	N5	N5	ZO	P5	P5

AFS Controller

AFS fuzzy controller calculates δ_{corr} based on δ and $e(\dot{\psi})$. As illustrated in Fig. 6, five membership functions are set for δ , and $e(\dot{\psi})$, which are two trapezoidal and three triangle membership functions. On the other hand, eleven membership functions are selected to represent the corrective steering angle as output of the controller, which is two trapezoidal, and nine triangle membership functions. The five symbols for the $\delta, e(\dot{\psi})$ are (HN), (LN), (ZO), (LP), (HP). The eleven variables for the corrective steering angle are (N5, N4, N3, N2, N1, ZO, P1, P2, P3, P4, and P5). The universe of discourse for the inputs was chosen based on their operating range. The corrective steering angle from fuzzy control is obtained with a scaling factor. The rule base of the AFS Fuzzy controller is the same as ESC is given in Table 2.

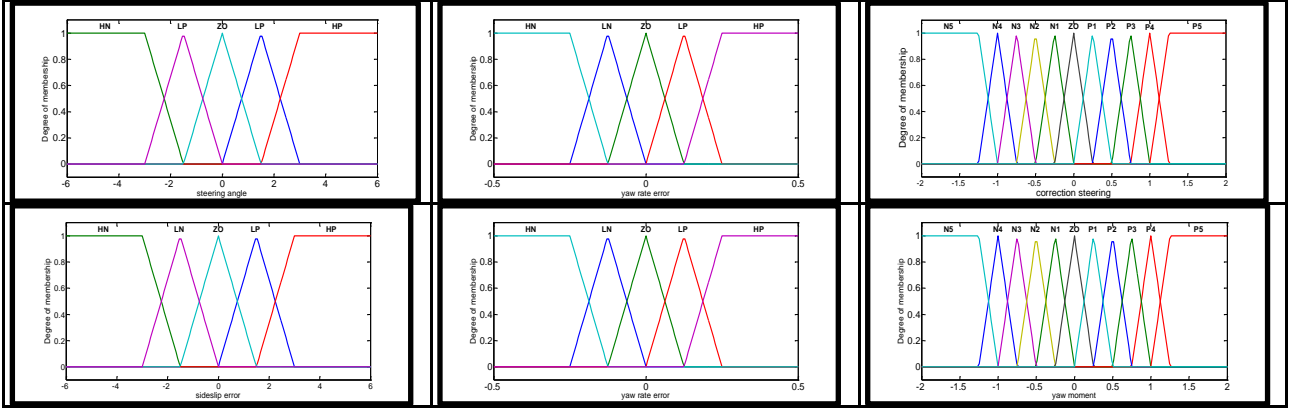


Fig. 4 Memberships function of ESC and AFS

AS Controller

The proposed active suspension control strategy consists of feedback FLC and feedforward FLC as presented in Fig.3. The inputs of feedforward FLC are δ, \dot{x} and the output is feedforward active roll moment $M_{\phi ff}$. The inputs for the feedback FLC are $(e(\phi), \frac{d}{dt}e(\phi))$ and the output is the feedback active roll moment $M_{\phi fb}$. The resultant active roll moment (M_{ϕ}) which is the summation of the both ($M_{\phi ff}$) and $M_{\phi fb}$.

As demonstrated in Figs. 4-5 Gaussian membership functions were chosen due to their smooth mapping property for control to represent the inputs and output variables for both controllers.

Feedforward FLC as shown in Fig.4 used seven Gaussian memberships for δ , five Gaussian membership functions for \dot{x} , and seven Gaussian memberships functions for $M_{\phi ff}$. The symbols for seven variables for δ , and $M_{\phi ff}$ are high negative (HN), medium negative (MN), low negative (LN), zero (Zo), low positive (LP), medium positive (MP), and high positive (HP). The symbols for \dot{x} are x_1, x_2, x_3, x_4, x_5 , the rule base between the inputs and the output is tabulated in Table 3.

Feedback FLC as shown in Fig.5 used five Gaussian membership functions for $(e(\phi), \frac{d}{dt}e(\phi), M_{\phi fb})$, which are medium negative (MN), low negative (LN), zero (ZO), low positive (LP), and medium positive (MP), the rule base between the inputs and the output is tabulated in see Table 4. The active roll moment was normalized in the range [-1 1] and then converted to suspension actuators according to the following equation:-

$$M_{\phi} = \frac{t_{rf}}{2} (F_{cfl} - F_{cfr} + F_{crl} - F_{crr}) \tag{17}$$

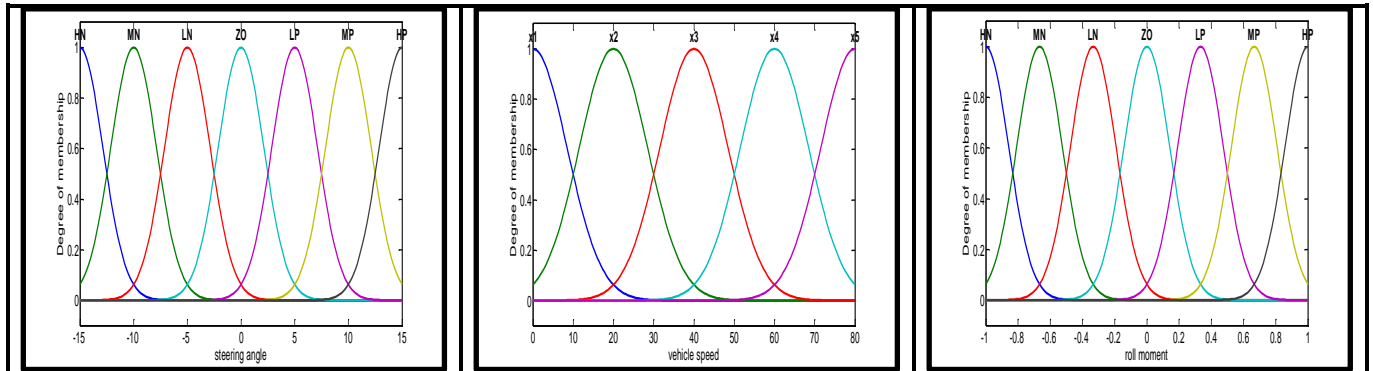
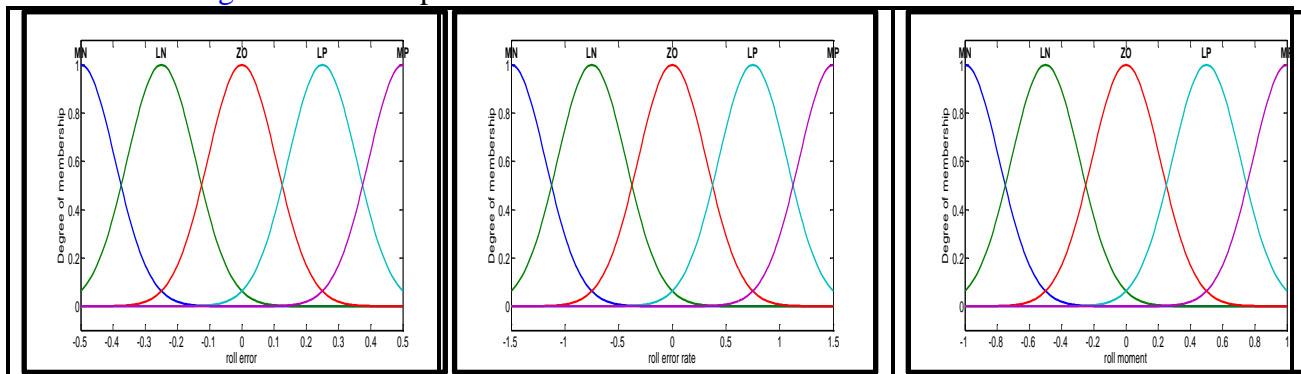
F_a is the actuator force at each corner of the vehicle.

Table 3. Rule Base for Feedforward Fuzzy Logic Controller

Speed/steering	HN	MN	LN	ZO	PS	PM	PL
X_1	ZO						
X_2	MN	MN	MN	ZO	MP	MP	PM
X_3	LN	MN	MN	ZO	MP	MP	HP
X_4	LN	LN	LN	ZO	HP	HP	HP
X_5	LN	LN	LN	ZO	HP	HP	HP

Table 4. Rule Base for Feedback Fuzzy Logic Controller

Roll error/roll error rate	MN	LN	ZO	LP	MP
MN	MN	MN	MN	MP	MP
LN	MN	LN	LN	LP	MP
ZO	MN	LN	ZO	LP	MP
LP	MN	LN	LP	LP	MP
MP	MN	MN	MP	MP	MP

**Fig. 5** Memberships function of the feedforward roll moment controller**Fig. 6** Memberships function of the feedback roll moment controller

Coordinated Controller

The objective of the coordinated (supervisor) controller is to manage AFS, ESC, and AS controllers in order to achieve a degree of performance that would not otherwise be possible by combined them together. The combined controller was based primarily on vehicle yaw velocity, vehicle side-slip angle, and roll angle errors, derived from the actual and desired values. A coordinator FLC based on lateral acceleration value is designed to coordinate among individual control systems as illustrated in Fig. 7. The lateral acceleration acting as input to the coordinator FLC, which is represented by three member ship functions namely low, medium, and high, on the other hand the outputs are three gain factors for each active system (AFS, AS and ESC). AFS gain factor as output is symbolized by three Gaussian member ship functions, which are low, medium, and high. The same for ESC gain factor and AS gain factor as outputs, but represented by two Gaussian member ship functions, which are low, and high, all the member ship functions are illustrated in Fig. 8. The switch gain function of control authority between individual control systems takes place using a defined rule base as follow:

1. IF the lateral acceleration is "low" THEN AFS is "high", and ESC is "low", and AS is "low".
2. IF the lateral acceleration is "low" THEN AFS is "high", and ESC is "low", and AS is "low".
3. IF the lateral acceleration is "low" THEN AFS is "high", and ESC is "low", and AS is "low".

Model Simulation

A numerical simulation study is accompanied to indicate the efficiency of the coordinate controller, and comparing with the combined controller. The 14-DOF All-Wheel-Drive full vehicle model is developed and simulated in MATLAB/ Simulink environment. The necessary parameters required by the vehicle model are given in [Appendix A](#). The fuzzy logic controller is designed using the fuzzy logic toolbox in MATLAB/Simulink. The effects of the coordinate controller, combined controller, and without controller in vehicle dynamics are shown. The efficiency of the controllers is shown considering three different standard cornering test maneuvers at different high vehicle forward velocity of 30 and 40 m/s namely: J-turn maneuver, fishhook maneuver, and double lane change maneuvers as shown in [Fig. 9](#).

Results and Discussion

Using continuous time simulation, the simulation results are performed for a three different maneuvers namely, J turn, fishhook, and double lane change at a high vehicle forward velocity of 30 and 40 m/s respectively with a nominal road friction coefficient of $\mu=0.9$, a rate considered to be normally illustrative of dry pavement.

The response of uncontrolled, combined control, and coordinated control are shown for five stability performances indices which are lateral acceleration, roll angle, side slip angle, yaw rate, and dynamic load transfer ratio which is only for fishhook maneuver only with high forward vehicle velocity of 30 and 40 m/s respectively. In all cases, without a controller the vehicle stability performance indices are too large and oscillate.

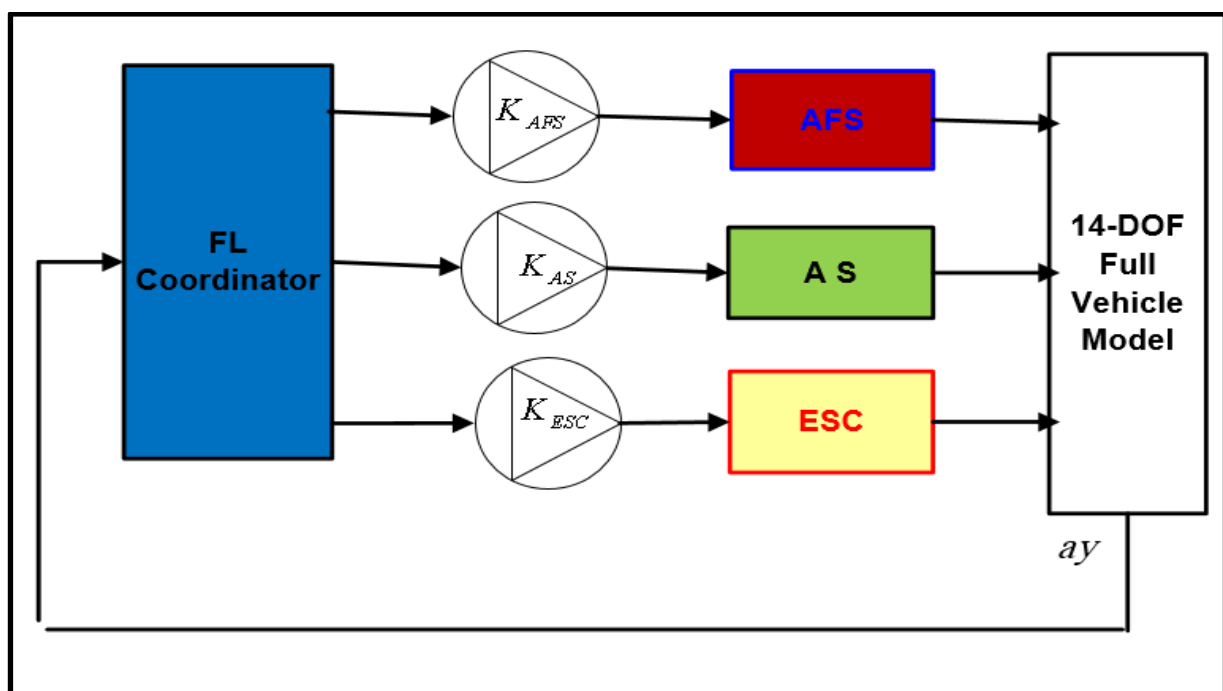


Fig. 7 Block diagram of the coordinated controller

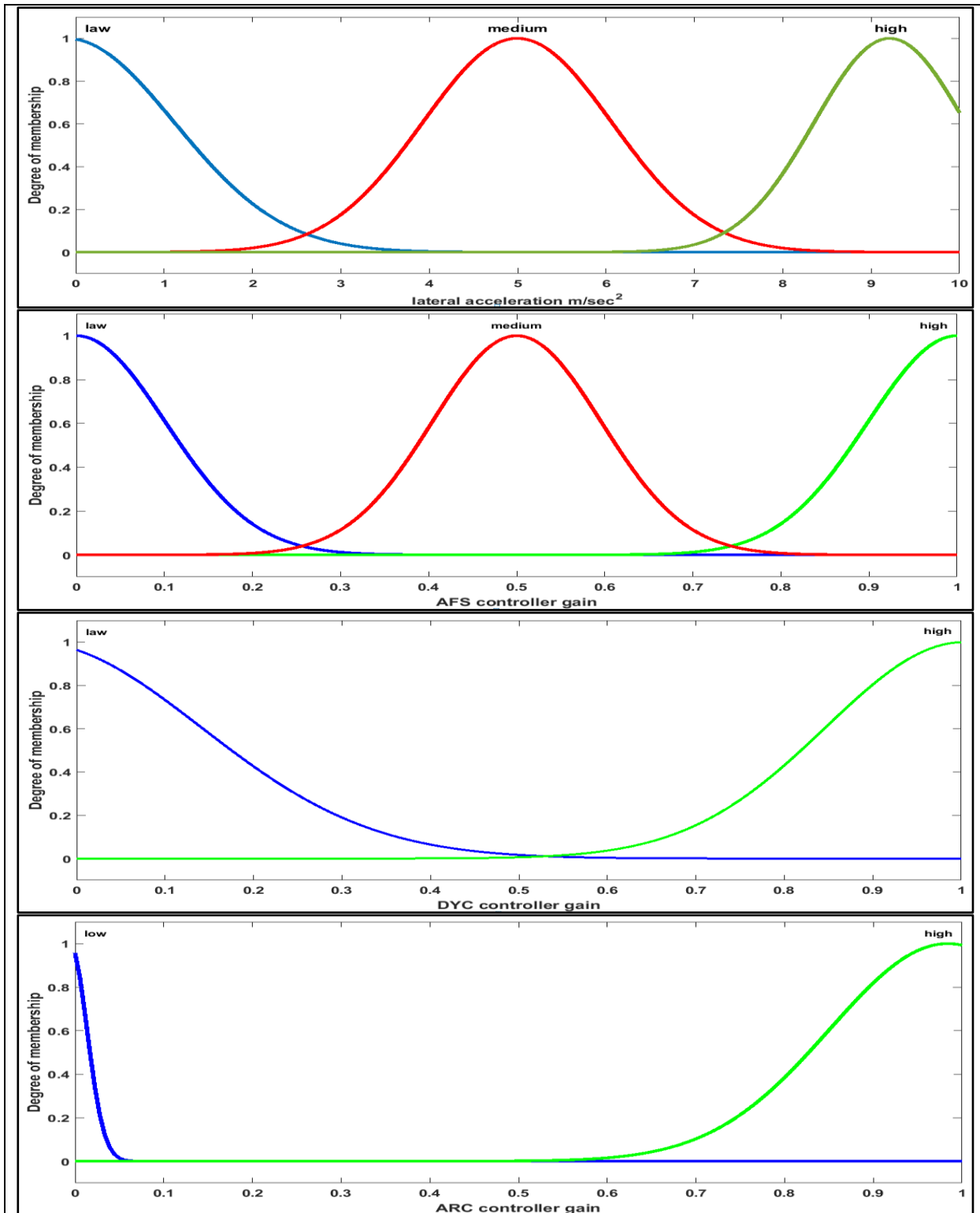


Fig. 8 Memberships function of the coordinator controller

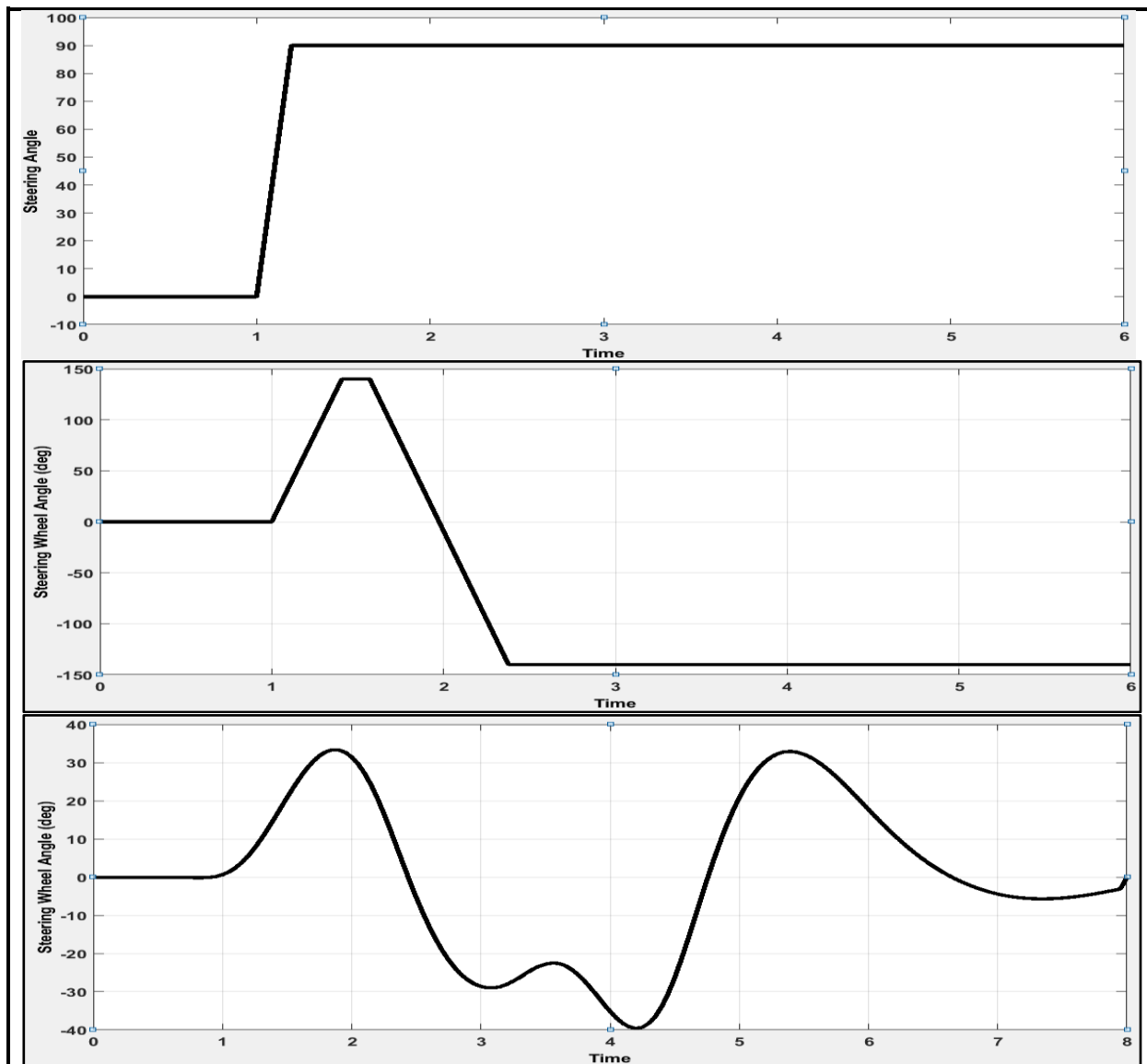


Fig. 9 Three standards different driver steering input (degree)

J-turn maneuver

Figs. 10-11 show the vehicle response for uncontrolled system, combined control, and coordinated control during J-turn maneuver with maximum angle of 90 degree at speed 30 and 40 m/s respectively.

In Fig. 10 the coordinated control more powerful than combined control, especially in tracking the desired value of the lateral acceleration, and yaw rate. The root mean square values of the uncontrolled system, combined controller, and coordinated controller are tabulated in Table 5, showing the improvement in percentage of the coordinated control better than the combined control, and the improvement in the sideslip angle is the best.

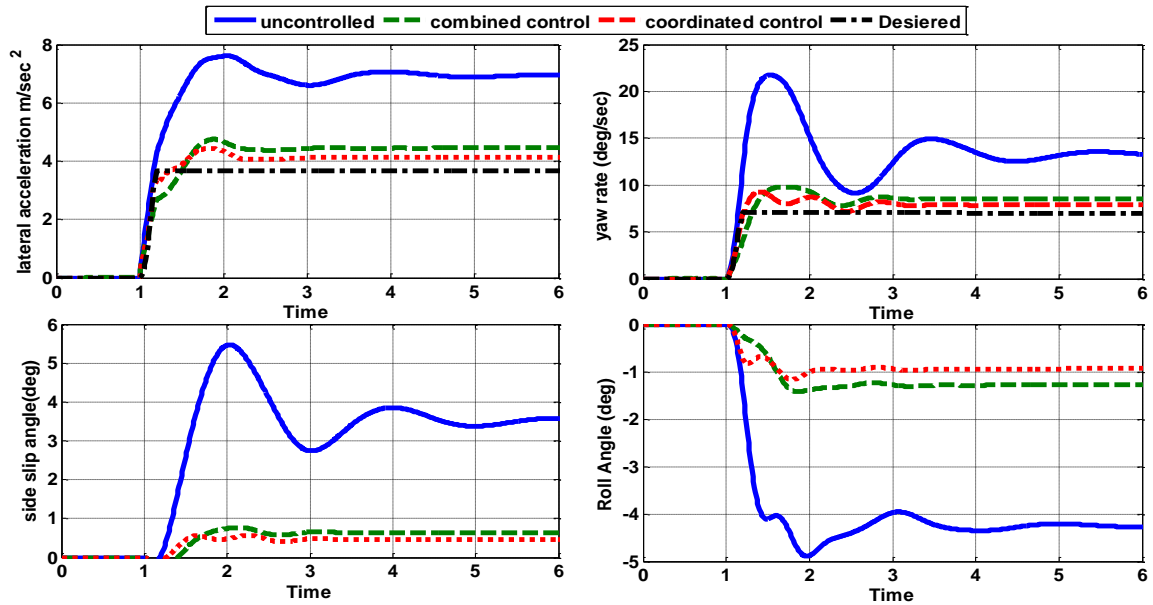


Fig. 10 Vehicle response during J- turn with speed 30 m/s

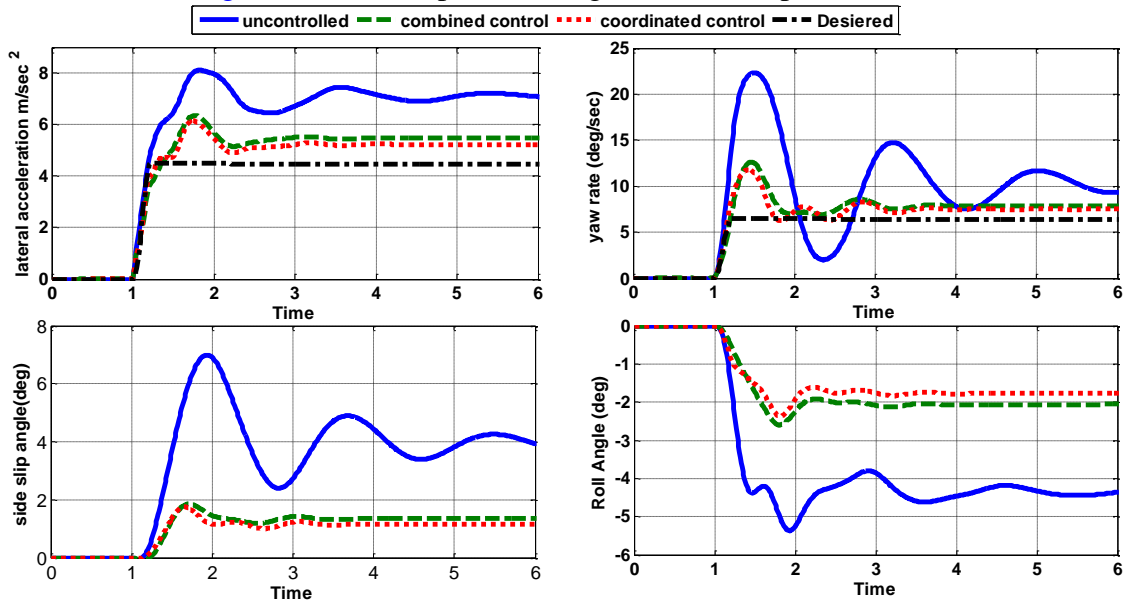


Fig. 11 Vehicle response during J- turn with speed 40 m/s

Table 5. RMS for J-turn Steer test at 30 m/s

Criteria	uncontrolled	Combined control	Coordinated control
Lateral acceleration	6.5037	4.1433 (36.3%)	3.8714 (40.4%)
Side slip angle	3.3844	0.5942 (82.4%)	0.4331 (87.2%)
Yaw rate	12.9544	8.0083 (38.2%)	7.4649 (42.3%)
Roll angle	3.9857	1.1808 (70.3%)	0.8808 (77.2%)

In Fig. 11 the coordinated control is better than combined control, the root mean square values of the uncontrolled system, combined controller, coordinated controller are tabulated in Table 6, showing the improvement in percentage of the coordinated control less than the obtained in Table 5 due to high vehicle velocity.

Table 6. RMS for J-turn Steer test at 40 m/s

Criteria	uncontrolled	Combined control	Coordinated control
Lateral acceleration	6.6536	5.1310 (22.9%)	4.9093 (26.2%)
Side slip angle	3.8638	1.2577 (67.4%)	1.0965 (71.6%)
Yaw rate	10.4674	7.5386 (28%)	7.1952 (31.2%)
Roll angle	4.0846	1.9184 (53%)	1.6514 (59.5%)

Fishhook Maneuver

To demonstrate the effect of the coordinated control in preventing rollovers. The simulation is performed with steering input fishhook maneuver with maximum angle of 140 degree at speed 30 and 40 m/s respectively.

The simulation results are depicted in Figs 12-13, which are reflecting a remarkable improvement in vehicle handling, stability, and rollover prevention. In Fig. 12 the forward velocity of the vehicle is 30 m/s, the coordinated control almost as the same effect as combined control with slight Improvement in coordinated control as show in Table 7. In Fig. 13 the forward velocity of the vehicle is 40 m/s, it is the same behaviour obtained in Fig 12. The root mean square values of the uncontrolled system, coordinated control, and combined control for fishhook maneuver at 40 m/s are tabulated in Table 8

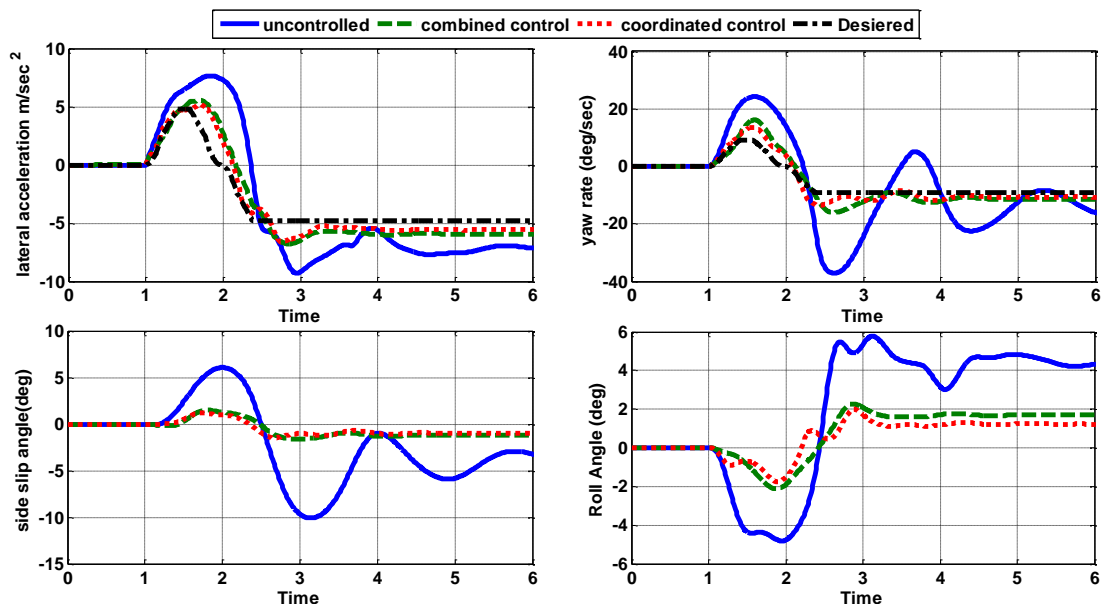


Fig. 12 Vehicle response during Fishhook- turn with speed 30 m/s

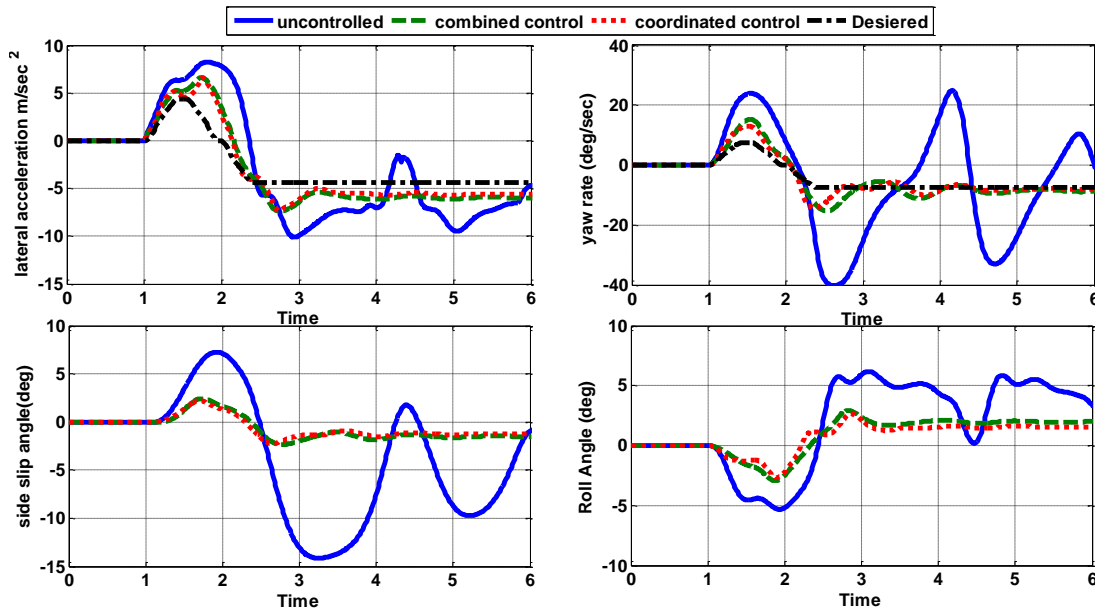


Fig. 13 Vehicle response during Fishhook- turn with speed 40 m/s

Table 7. RMS for Fish Hook Steer test at 30 m/s

Criteria	uncontrolled	Combined control	Coordinated control
Lateral acceleration	6.6793	5.3469 (19.9%)	5.0317 (24.6%)
Side slip angle	4.4147	1.1190 (74.6%)	0.9126 (79.3%)
Yaw rate	15.6534	10.6479 (31.9%)	9.9125 (36.7%)
Roll angle	4.1598	1.5397 (63%)	1.1358 (72.7%)

Table 8. RMS for Fish Hook Steer test at 40 m/s

Criteria	uncontrolled	Combined control	Coordinated control
Lateral acceleration	6.7133	5.466 (18.6%)	5.1306 (23.6%)
Side slip angle	6.2577	1.4472 (76.8%)	1.2352 (80.2%)
Yaw rate	16.3146	8.4386 (48.3%)	7.8255 (52%)
Roll angle	4.2293	1.8378 (56.5%)	1.4620 (65.4%)

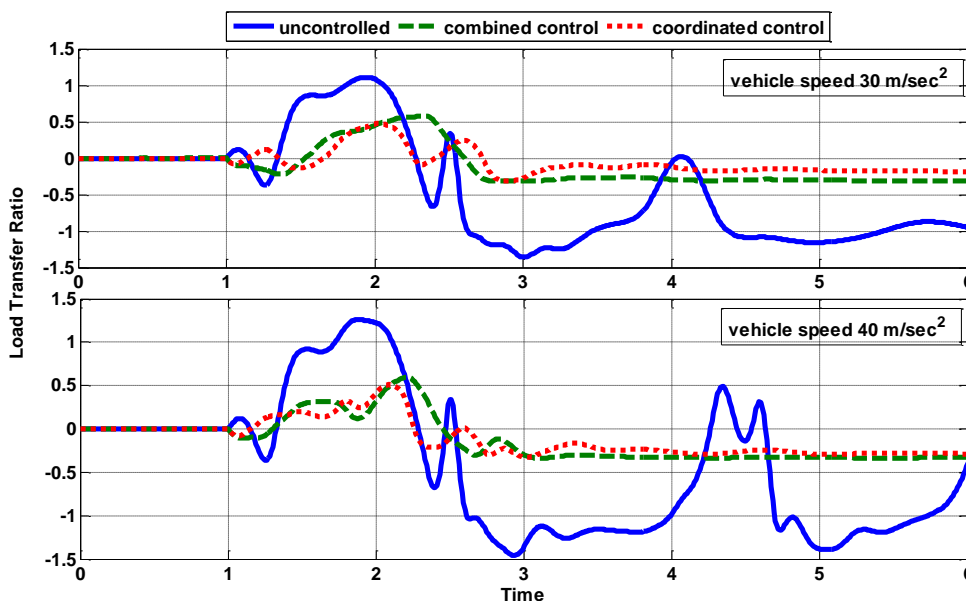


Fig. 14 Load transfer ratio during Fishhook steer test

As shown in Fig 14 the dynamic load transfer ratio is illustrated to study the effect of the proposed controller in rollover behaviour, it is clear that both the controllers avoid the wheel lift up with better performance for the coordinated control.

Double Lane-Change Maneuver

Four stability indices for double lane-change maneuver ISO 3888-2 (2002) are shown in Figs 15-16 at speed 30 and 40 m/s respectively for the all systems. It is clear that the coordinated control is better than combined control with a little improvement as tabulated in Table 9, and Table 10.

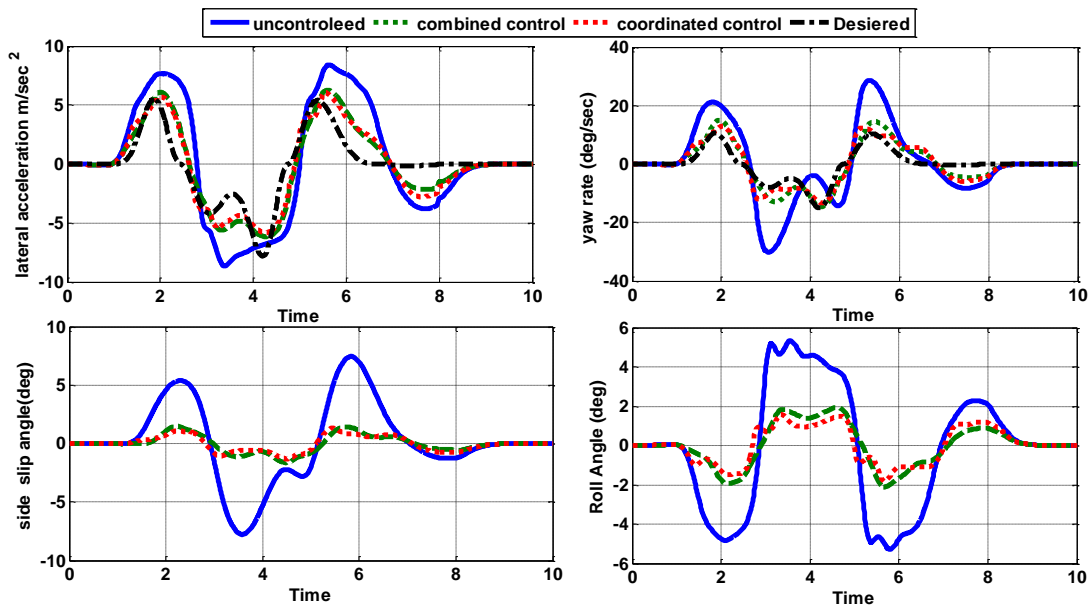


Fig. 15 Vehicle response during double lane change with speed 30 m/s

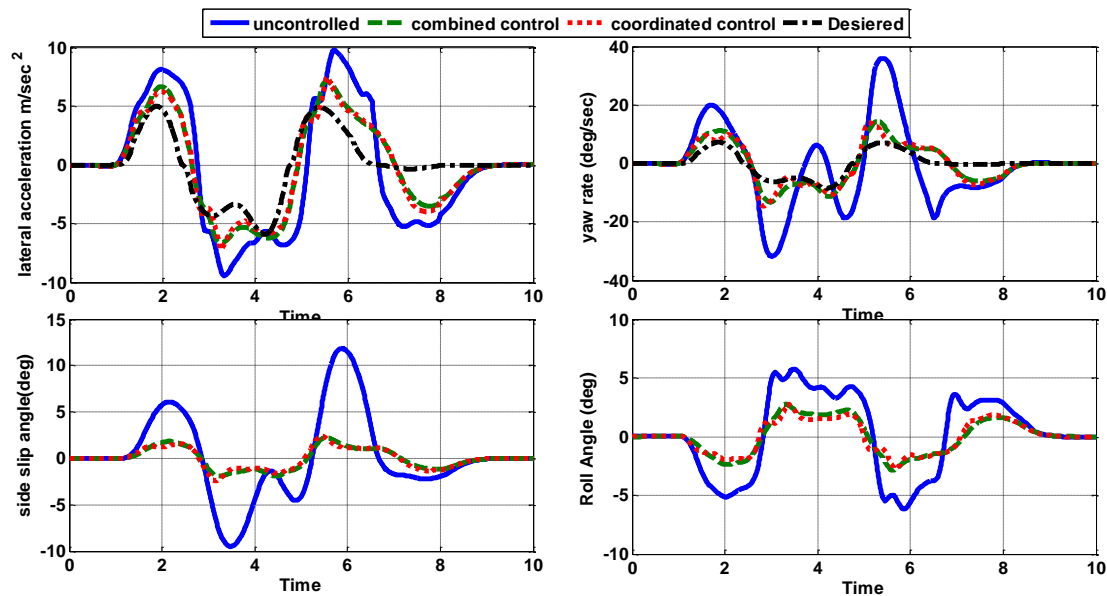


Fig. 16 Vehicle response during double lane change with speed 40 m/s

Table 9. RMS for Double Lane Change Steer test at 30 m/s

Criteria	uncontrolled	Combined control	Coordinated control
Lateral acceleration	4.9276	3.3317 (32.4%)	3.2437 (34.2%)
Side slip angle	3.4185	0.7205 (78.9%)	0.6354 (81.4%)
Yaw rate	12.5676	7.212 (42.6%)	6.8569 (45.4%)
Roll angle	3.1237	1.0726 (65.6%)	0.9259 (70.3%)

Table 10. RMS for Double Lane Change Steer test at 40 m/s

Criteria	uncontrolled	Combined control	Coordinated control
Lateral acceleration	5.2356	3.8257 (25%)	3.7327 (28.7%)
Side slip angle	4.5509	1.0923 (76%)	1.0733 (76.4%)
Yaw rate	13.5052	6.4964 (51.9%)	6.3450 (53%)
Roll angle	3.3463	1.4776 (55.8%)	1.3417 (59.9%)

The above simulation results show that a vehicle equipped with the coordinated control, and combined control can sustain its handling, stability, and rollover prevention in various hazardous conditions (different maneuvers) compared to the uncontrolled vehicle. In addition, the coordinated control system can improve the vehicle stability performance by maintain vehicle response more close to the desired path than the combined controller beside managing the different controllers and minimizing the energy consumed.

Conclusions

The presented paper proposed a coordinated control system that manages (AFS), (ESC), and (AS) with supervisor FLC depending on the value of the lateral acceleration as input to the FLC to enhance the vehicle handling, stability, and rollover prevention. The proposed coordinated control system organizes the weighting of each control through different lateral acceleration that represents the most of the maneuvers situations.

The efficiency of the suggested coordinated control has been assessed through the mathematical modeling of a vehicle using MATLAB/Simulink. The fuzzy logic method based controller is shown to be an effective means of controlling vehicle stability, handling, and rollover prevention. The simulation results show that the coordinated control is more effective than combined control in points of put the vehicle on its desired values of lateral acceleration, and yaw rate. Also minimize the value of the roll angle, side slip angle, and dynamic load transfer ratio, with taking in consideration to minimize the conflict between different active system, and save energy consumption.

References

1. Li, L., et al., A novel fuzzy logic correctional algorithm for traction control systems on uneven low-friction road conditions. *Vehicle System Dynamics*, 2015. **53**(6): p. 711-733.
2. Mammarr, S. and D. Koenig, *Vehicle handling improvement by active steering*. *Vehicle system dynamics*, 2002. **38**(3): p. 211-242.
3. Chen, Y., J.K. Hedrick, and K. Guo, *A novel direct yaw moment controller for in-wheel motor electric vehicles*. *Vehicle System Dynamics*, 2013. **51**(6): p. 925-942.
4. Yamakado, M., K. Nagatsuka, and J. Takahashi, *A yaw-moment control method based on a vehicle's lateral jerk information*. *Vehicle System Dynamics*, 2014. **52**(10): p. 1233-1253.
5. Hartikainen, L., F. Petry, and S. Westermann, *Longitudinal wheel slip during ABS braking*. *Vehicle System Dynamics*, 2015. **53**(2): p. 237-255.
6. Tchamna, R., E. Youn, and I. Youn, Combined control effects of brake and active suspension control on the global safety of a full-car nonlinear model. *Vehicle System Dynamics*, 2014. **52**(sup1): p. 69-91.
7. Hac, A. and M.O. Bodie, *Improvements in vehicle handling through integrated control of chassis systems*. *International journal of vehicle autonomous systems*, 2002. **1**(1): p. 83-110.
8. Gordon, T., M. Howell, and F. Brandao, *Integrated control methodologies for road vehicles*. *Vehicle System Dynamics*, 2003. **40**(1-3): p. 157-190.
9. Selby, M.A., *Intelligent vehicle motion control*. 2003, University of Leeds.
10. Trachtler, A., Integrated vehicle dynamics control using active brake, steering and suspension systems. *International Journal of Vehicle Design*, 2004. **36**(1): p. 1-12.
11. He, J., et al., *Coordination of active steering, driveline, and braking for integrated vehicle dynamics control*. *Proceedings of the Institution of Mechanical Engineers, Part D: Journal of Automobile Engineering*, 2006. **220**(10): p. 1401-1420.
12. Lu, S.-B., et al., Integrated control on MR vehicle suspension system associated with braking and steering control. *Vehicle System Dynamics*, 2011. **49**(1-2): p. 361-380.
13. Rengaraj, C. and D. Crolla, Integrated chassis control to improve vehicle handling dynamics performance. 2011, SAE Technical Paper.
14. Song, P., M. Tomizuka, and C. Zong, *A novel integrated chassis controller for full drive-by-wire vehicles*. *Vehicle System Dynamics*, 2015. **53**(2): p. 215-236.
15. Alberding, M.B., J. Tjønnås, and T.A. Johansen, Integration of vehicle yaw stabilisation and rollover prevention through nonlinear hierarchical control allocation. *Vehicle System Dynamics*, 2014. **52**(12): p. 1607-1621.
16. Sharaf, A., *Real-time assessment of vehicle response in a virtual proving ground*. *International Journal of Heavy Vehicle Systems*, 2013. **20**(2): p. 174-189.
17. Ellis, J.R., *Vehicle handling dynamics*. 1994.
18. Pacejka, H., *Tire and vehicle dynamics*. 2005: Elsevier.
19. Rajamani, R., *Vehicle dynamics and control*. 2011: Springer Science & Business Media.
20. Zhang, Y., A. Khajepour, and X. Xie, *Rollover prevention for sport utility vehicles using a pulsed active rear-steering strategy*. *Proceedings of the Institution of Mechanical Engineers, Part D: Journal of Automobile Engineering*, 2015: p. 0954407015605696.